$R_2NBNR_2^+$ ($\nu_{as}(BN_2)$ 1956 cm^{-1} [6]). In most cases, we observe a fairly strong band in the 1200–1300-cm^{-1} region, which we believe to be associated with $\nu_{as}(BeN_2)$.

Mass spectra of **1–4**, taken at 15 and 70 eV, show no general pattern. Surprisingly, the intensity of the molecular ion was weak in all cases, an (M − 15) peak usually being the base peak. Only M^+ of **3** had a fairly high intensity (11% at 70 eV). The beryllium atom is readily removed in the fragmentation process by breaking the BeN bond with formation of R_2N^+, R_2NH^+, and $SiMe_3^+$ and further fragmentation of these species. Again, **3** provides an exception, insofar, as fragments in the ranges *m/e* 274–276, 258–260, and 149–151 contain Be, as shown by good agreement between observed and calculated peak patterns. Interestingly, M^+ of dimeric **2** is quite intense (25%), and the molecular ion decomposes in two ways: (i) by fragmentation into M^+ of monomeric **2**, ascertained by a metastable peak, and (ii) by cleavage of one BeN bond, leading to a fragment of *m/e* 318. The base peak in this case is $(M - 15)^+$ of monomeric **2**.

Chemical Behavior

1–4 are quite susceptible to hydrolysis with formation of $Be(OH)_2$ and the amine. They are, however, stable toward oxygen at room temperature.

The compounds can be readily mixed with ether, tetrahydrofuran, monoglyme, and diglyme, and ^9Be NMR shows that these ethers will not coordinate. Also, **1–4** dissolve in hexane, cyclohexane, benzene, and toluene. Again, neither $\delta(^9Be)$ nor the line width is affected.

In contrast, **2** reacts with pyridine only, forming a deep red solution in benzene or cyclohexane. Although we have been unable to isolate an analytically pure adduct, NMR data provide strong evidence for a 1:1 adduct: the ^9Be signal is shifted to 11.5 ppm, $h_{1/2}$ = 155 Hz, data typical for tricoordinate beryllium. Both data remain virtually unaffected on adding more pyridine, and the same holds for the ^1H NMR spectrum ($\delta(^1H)$ 1.10 doublet, 3.40 septet, 6.68, 7.04, 8.50). The signals for pyridine are somewhat broad and are further broadened on adding pyridine, thus indicating pyridine exchange at the recording temperature. This result indicates that monomeric beryllium bis(amides) are weak Lewis acids and electrophiles. They are generally not susceptible to transamination with secondary amines due to steric hindrance. However, the action of pyridine on **2** suggests that less bulky amines such as primary amines and ammonia will interact, especially with **2**, the least sterically hindered monomeric $Be(NR_2)_2$, and some preliminary data support this expectation.[17]

Conclusion

There is obviously a close relationship between the existence of monomer bis(alkylamido)beryllium compounds and bis(dialkylamido)boron cations because each of the beryllium amides **1–4** reported here has an isoelectronic and isotructural counterpart $(R_2N)_2B^+$ (R_2N = N-*i*-Pr_2;[5] tmp, NEt_2,[6] N-$(SiMe_3)_2$;[18] $NCMe_3SiMe_3$[18]). It will, therefore, be interesting to see whether it is possible to also prepare and investigate monomeric beryllium amides of type $RBeNR_2$, formally possessing an electron sextet structure in analogy to $R'BNR_2^+$.[6] Some of these boron cations with bulky R′ groups are stable in solution for a short while even at room temperature.[18]

Acknowledgment. The support of this work by the Deutsche Forschungsgemeinschaft and Fonds der Chemischen Industrie is gratefully acknowledged.

Registry No. **1**, 25733-02-2; **2**, 86563-54-4; $[\mathbf{2}]_2$, 86563-58-8; **3**, 86563-55-5; **4**, 86563-56-6; $[\mathbf{5}]_3$, 86563-57-7; $BeCl_2$·HN-*i*-Pr_2, 86568-70-9.

(18) H. Nöth and S. Weber, unpublished work, 1982.

Contribution from the Instituto de Quimica, Universidade de Sao Paulo, Sao Paulo, Brazil, and the Department of Chemistry, University of Missouri, Columbia, Missouri 65211

Pentacyanoferrate(II) Complexes of Pyrimidine and Quinoxaline

AUGUSTO L. COELHO, HENRIQUE E. TOMA, and JOHN M. MALIN*[1]

Received February 10, 1983

The ions pentacyano(pyrimidine)ferrate(II) and pentacyano(quinoxaline)ferrate(II) have been characterized in aqueous solution. The complexes exhibit strong metal-to-ligand charge-transfer absorptions respectively at 410 nm (ϵ_{max} = 3.1 × 10^3 M^{-1} cm^{-1}) and 545 nm (6.0 × 10^3 M^{-1} cm^{-1}). In the presence of excess heterocycle, the rate law for formation of the complexes from pentacyanoaquaferrate(II) ion is $d[Fe(CN)_5L^{2-}]/dt = k_f[Fe(CN)_5OH_2^{3-}][L]$. For the pyrimidine reaction, k_f = 340 ± 25 M^{-1} s^{-1} (25 °C, 0.10 M ($LiClO_4$)), $\Delta H^{\ddagger}$ = 15.5 ± 1 kcal mol^{-1}, and $\Delta S^{\ddagger}$ = 6 ± 3 cal mol^{-1} deg^{-1}. In the quinoxaline case, k_f = 425 ± 25 M^{-1} s^{-1}, $\Delta H^{\ddagger}$ = 15.2 ± 1 kcal mol^{-1}, and $\Delta S^{\ddagger}$ = 6 ± 3 cal mol^{-1} deg^{-1}. Ligand-exchange studies yielded values for the specific rates of dissociation. For the pyrimidine complex, k_d = (1.3 ± 0.1) × 10^{-3} s^{-1}, $\Delta H^{\ddagger}$ = 21.8 ± 2 kcal mol^{-1}, and $\Delta S^{\ddagger}$ = 2 ± 6 cal mol^{-1} deg^{-1}. For quinoxaline, k_d = 0.62 ± 0.10 s^{-1}, $\Delta H^{\ddagger}$ = 19.6 ± 2 kcal mol^{-1}, and $\Delta S^{\ddagger}$ = 4 ± 6 cal deg^{-1} mol^{-1}. One-electron oxidation of the complexes by cyclic voltammetry is reversible, with E_f = −0.52 and −0.55 ± 0.03 V vs. NHE, respectively, for the pyrimidine and quinoxaline complexes. The stabilities of the iron(III) complexes can be estimated from the electrochemical results and ligand substitution properties of the iron(II) species.

Introduction

The chemistry of substituted pentacyanoferrate(II) complexes, $Fe(CN)_5L^{3-}$, where L represents an aromatic N-heterocycle, saturated amine, or other donor ligand, has proved to be a rich source of information about metal–ligand interactions. Initially undertaken to probe for $d\pi$–$p\pi$ back-bonding between Fe(II) and various ligand systems, studies of $Fe(CN)_5L^{3-}$ species have produced a number of new complex ions whose spectra and photochemical and electrochemical properties are of significance and utility.[2-16]

(1) Present address: c/o Petroleum Research Fund, American Chemical Society, Washington, DC 20036.
(2) Larue, T. A. *Anal. Chim. Acta* **1968**, *40*, 437.

0020-1669/83/1322-2703$01.50/0 © 1983 American Chemical Society

In this paper report the characterization of the pentacyanoferrate(II) complexes of aromatic N-heterocycles pyrimidine (pyr, I) and quinoxaline (qx, II). The complexes are

I II

of interest because their properties reflect the influences of steric and electronic interactions upon metal–ligand bond strengths. Also, both ligands are potential bridging groups capable of mediating electron transfer in binuclear "precursor" complexes.[13] Finally, the new species reported here form a basis for comparison with the biologically important purine and pyrimidine bases.

Experimental Section

The starting material sodium pentacyanoammineferrate(II) trihydrate was prepared as described previously.[17] Anal.[18] Calcd for $C_5N_6H_9O_3FeNa_3$: C, 18.24; H, 2.78; N, 25.78. Found: C, 18.18; H, 2.84; N, 25.71. Ligands pyrimidine and quinoxaline were purchased from Aldrich Chemical Co. and used without further purification. Lithium perchlorate solutions of known concentration were added to experimental solutions in order to maintain ionic strength. Doubly distilled water was employed in all the experiments.

A Durrum Model D-110 stopped-flow instrument was used for the rapid kinetics experiments. Visible–UV spectra were obtained by employing Cary Model 17 and 14 spectrophotometers. Temperature control in the cuvettes was ±0.3 °C. Cyclic voltammetry experiments were performed with the PAR equipment described previously.[10] Rate constants were computed from absorbance vs. time data by methods that have been described.[13] For the rate measurements, aqueous solutions of the pentacyanoaquaferrate(II) complex (ca. 10^{-5} M) were freshly prepared and used within the first 0.5 h to avoid complications due to the aging process associated with the pentacyanoaquaferrate(II) ion.[3]

Results

Characterization of the Complexes. The pentacyanoaquaferrate(II) ion, generated by facile aquation of the pentacyanoammineferrate(II) species ($t_{1/2}$ = 40 s),[15] reacts readily with the free bases quinoxaline and pyrimidine. The adducts absorb light strongly, exhibiting nearly Gaussian-shaped metal-to-ligand charge-transfer (MLCT) bands in the visible region. For the quinoxaline complex, λ_{max} is located at 545 nm, while ϵ_{max} is (6.0 ± 0.4) × 10^3 M^{-1} cm^{-1}. For the pyrimidine complex these quantities are respectively 410 nm and (3.1 ± 0.1) × 10^3 M^{-1} cm^{-1}. Normally the complexes were studied in the presence of a large excess of the organic ligand. Under the conditions of the experiment the formation of complexes of other than 1:1 stoichiometry was thought to be extremely unlikely. Nonetheless, a Job plot was constructed for the pyridine system to determine whether a complex of Fe:pyr ratio 2:1 might be detected.[19] The experiment, employing a total concentration of Fe(II) plus ligand equal to 3.5 × 10^{-4} M, showed conclusively that the only complex formed is of 1:1 stoichiometry. For the quinoxaline system the formation constant of the 1:1 complex was found to be relatively low (ca. 10^2 M^{-1}). It is improbable that a 2:1 species would be detectable under the conditions of this work. In the course of the kinetics studies, no evidence could be found that indicated in any way the presence of a binuclear complex for either quinoxaline or pyrimidine.

Protonation of Pentacyano(pyrimidine)ferrate(II). The MLCT band of the pyrimidine complex was found to be shifted to shorter wavelengths when the solution pH was lowered from 7 to 2. This behavior has been observed in other pentacyanoferrate(II) complexes, and it is explained by reaction 1

$$H^+ + (NC)_5FeL^{3-} \rightleftharpoons H(NC)_5FeL^{2-} \quad (1)$$

is protonated at cyanide.[3] Spectrophotometric titrations of the pyrimidine complex showed clear isosbestic behavior, indicating that only the singly protonated and deprotonated forms of the chromophore were present. The data yielded pK_a = 2.65 (25 °C, μ = 0.10 M), employing computational methods described previously.[3] The pK_a value agrees closely with that measured for $H(NC)_5FeOH_2^{2-}$ (pK_a = 2.63, μ = 0.10 M)[21] but is somewhat higher than the values found for other substituted pentacyanoferrate(II) species measured at higher ionic strength (pK_a = 2.0–2.2, μ = 1.0 M).[3] The protonation experiment could not be performed with the quinoxaline complex because of its instability.

Kinetics of Formation of the Pentacyano(quinoxaline)ferrate(II) Complex. Because of its relative lability to substitution, the reactions of both formation and dissociation of the quinoxaline complex could be studied by the stopped-flow technique. Biphasic plots of absorbance vs. time were observed after rapid mixing of a solution containing pentacyanoaquaferrate(II) with one containing both quinoxaline (qx) and dimethyl sulfoxide (Me_2SO) in water. The plots showed a rapid increase in absorption near 545 nm, followed by a decrease that was slower than the first phase by a factor of ca. 50. During the absorbance increase the observed pseudo-first-order rate constant arose from parallel reactions 2 and 3. The observed rate constant for the process is expressed by eq 4.

$$Fe(CN)_5OH_2^{3-} + qx \xrightarrow{k_2} Fe(CN)_5qx^{3-} + H_2O \quad (2)$$

$$Fe(CN)_5OH_2^{3-} + Me_2SO \xrightarrow{k_3} Fe(CN)_5Me_2SO^{3-} + H_2O \quad (3)$$

$$k_{f'} = k_2[qx] + k_3[Me_2SO] \quad (4)$$

The secondary, slow absorbance decrease corresponded to eq 5, the relatively reactive quinoxaline species was trans-

$$Fe(CN)_5qx^{3-} + Me_2SO \xrightarrow{k_{d'}} Fe(CN)_5Me_2SO^{3-} + qx \quad (5)$$

formed into the inert dimethyl sulfoxide complex.[4] In Table I are presented the specific rates of both processes, measured

(3) Toma, H. E.; Malin, J. M. *Inorg. Chem.* **1973**, *12*, 1039.
(4) Toma, H. E.; Malin, J. M.; Giesbrecht, E. *Inorg. Chem.* **1973**, *12*, 2084.
(5) Katz, N. E.; Blesa, M. A.; Olabe, J. A.; Aymonino, P. *Inorg. Chem.* **1978**, *17*, 556.
(6) Shepherd, R. E. *J. Am. Chem. Soc.* **1976**, *98*, 3329. The MLCT spectrum of the pentacyano(pyrimidine)ferrate(II) complex was reported by: R. E. Shepherd at the 183rd National Meeting of the American Chemical Society, Las Vegas, NV, 1982.
(7) Sceesy, A. P.; Miller, S. S.; Haim, A. *Inorg. Chim. Acta* **1978**, *28*, 189.
(8) Toma, H. E.; Martins, J. M.; Giesbrecht, E. *J. Chem. Soc., Dalton Trans.* **1980**, 1612.
(9) Figard, J. E.; Petersen, J. P. *Inorg. Chem.* **1978**, *17*, 1059.
(10) Hrepic, N. V.; Malin, J. M. *Inorg. Chem.* **1979**, *18*, 409.
(11) Toma, H. E. *J. Chem. Soc., Dalton Trans.* **1980**, 471.
(12) Davies, G.; Garafalo, A. R. *Inorg. Chem.* **1981**, *20*, 3543.
(13) Malin, J. M.; Ryan, D. A.; O'Halloran, T. V. *J. Am. Chem. Soc.* **1978**, *100*, 2097.
(14) Toma, H. E.; Creutz, C. *Inorg. Chem.* **1977**, *16*, 545.
(15) Toma, H. E.; Malin, J. M. *Inorg. Chem.* **1974**, *13*, 1772.
(16) Malin, J. M.; Brunschwig, B. S.; Brown, G. M.; Kwan, K. S. *Inorg. Chem.* **1981**, *20*, 1438.
(17) Brauer, G. "Handbook of Preparative Inorganic Chemistry", 2nd ed.; Academic Press: New York, NY, 1965; p 1511.
(18) Microanalysis performed by Galbraith Analytical Laboratory, Inc., Knoxville, TN.
(19) Vosburgh, W. C.; Cooper, G. R. *J. Am. Chem. Soc.* **1941**, *63*, 437.
(20) Toma, H. E.; Malin, J. M. *Inorg. Chem.* **1973**, *12*, 2080.
(21) Malin, J. M.; Koch, R. C. *Inorg. Chem.* **1978**, *17*, 752.
(22) Wiberg, K. B.; Lewis, T. P. *J. Am. Chem. Soc.* **1971**, *92*, 7154.

Table I. Observed Rate Constants of Formation and Dissociation of the Pentacyano(quinoxaline)ferrate(II) Complex[a]

run	temp, °C	[qx], M	[Me_2SO], M	k_f', s^{-1}	k_d', s^{-1}
1	14.0	0.000	0.010	1.39[b]	
2	14.0	0.0050	0.100		0.155[c]
3	14.0	0.0049	0.010	2.80	0.090
4	14.0	0.0164	0.010	4.60	0.054
5	14.0	0.033	0.010	7.1	0.038
6	14.0	0.045	0.010	8.4	0.028
7	14.0	0.067	0.010	11.7	0.020
8	19.3	0.00	0.010	2.23[b]	
9	19.3	0.0050	0.100		0.319[c]
10	19.5	0.0049	0.010	4.7	0.180
11	19.3	0.0164	0.010	6.8	0.096
12	19.3	0.033	0.010	11.4	0.068
13	19.5	0.045	0.010	13.7	0.052
14	19.3	0.067	0.010	17.7	0.039
15	25.0	0.000	0.010	3.40[b]	
16	25.0	0.0050	0.100		0.59[c]
17	25.0	0.0049	0.010	7.4	0.343
18	25.0	0.0164	0.010	10.8	0.195
19	25.0	0.033	0.010	18.0	0.127
20	25.0	0.045	0.010	22.5	0.092
21	25.0	0.067	0.010	31.8	0.071
22	30.6	0.00	0.010	5.8[b]	
23	30.6	0.0050	0.100		1.13[c]
24	30.6	0.0049	0.010	12.5	0.63
25	30.6	0.0164	0.010	16.7	0.32
26	30.6	0.033	0.010	27.1	0.25
27	30.6	0.045	0.010	35.7	0.19
28	30.5	0.067	0.010	48.5	0.16

[a] Conditions: μ = 0.10 M ($LiClO_4$), pH 7–8, [$Fe(CN)_5OH_2^{3-}$] = 1×10^{-5} M. [b] Formation of the pentacyano(dimethyl sulfoxide)-ferrate(II) complex. [c] Starting initially with the qunoxaline complex (10^{-5} M) in excess free heterocycle (5.0×10^{-3} M).

in the 14–30 °C range, pH 7–8, μ = 0.10 M ($LiClO_4$), at a fixed concentration of Me_2SO (0.010 M) and at concentrations of quinoxaline varying from 5.0×10^{-3} to 6.7×10^{-2} M. At each temperature one run, monitored at ca. 400 nm, was made to determine the specific rate of the Me_2SO reaction under the conditions used. These are runs 1, 8, 15, and 22.

Plots of k_f' for the formation reaction vs. the concentration of quinoxaline are given in Figure 1A. From the slopes of these plots, we have calculated k_2, the second-order specific rate for formation of the quinoxaline complex. Values obtained at various temperatures in the range 6–35 °C provided activation parameters. At 25 °C, k_2 is 425 ± 25 M^{-1} s^{-1}. $\Delta H^{\ddagger}$ is 15.2 ± 1 kcal/mol and $\Delta S^{\ddagger}$ equals 6 ± 3 cal mol^{-1} K^{-1}. In Figure 1A, the extrapolations of specific rates to low [qx] give nonzero ordinate intercepts. The solid-line (linear) extrapolations indicate the contributions of the Me_2SO substitution reaction, eq 3, to the measured specific rates. In the experiments, a deviation from linearity, shown in Figure 1A at low [qx], was observed. This may be because formation and dissociation of the quinoxaline complex are not completely separable at low [qx].

Dissociation Kinetics of the Quinoxaline Complex. Ligand substitution in aqueous pentacyanoferrate(II) complexes appears to occur by a dissociative process in which the rate-determining step is breakage of the metal–ligand bond.[3] For the quinoxaline complex in reaction with Me_2SO, the most likely mechanism is given by eq 6 and 7. A k_7 step is omitted

$$Fe(CN)_5qx^{3-}(aq) \underset{k_{-6}}{\overset{k_6}{\rightleftharpoons}} Fe(CN)_5OH_2^{3-} + qx \qquad (6)$$

$$Fe(CN)_5OH_2^{3-} + Me_2SO \xrightarrow{k_7} Fe(CN)_5Me_2SO^{3-}(aq) + H_2O \qquad (7)$$

because the Me_2SO complex dissociates at a negligible rate on the time scale of the experiment. With employment of the steady-state approximation and eq 6 and 7, the observed, pseudo-first-order rate of dissociation ($k_{d'}$) is given by eq 8 and 9. Plots of k_d^{-1} vs. [qx] are given in Figure 1B. From

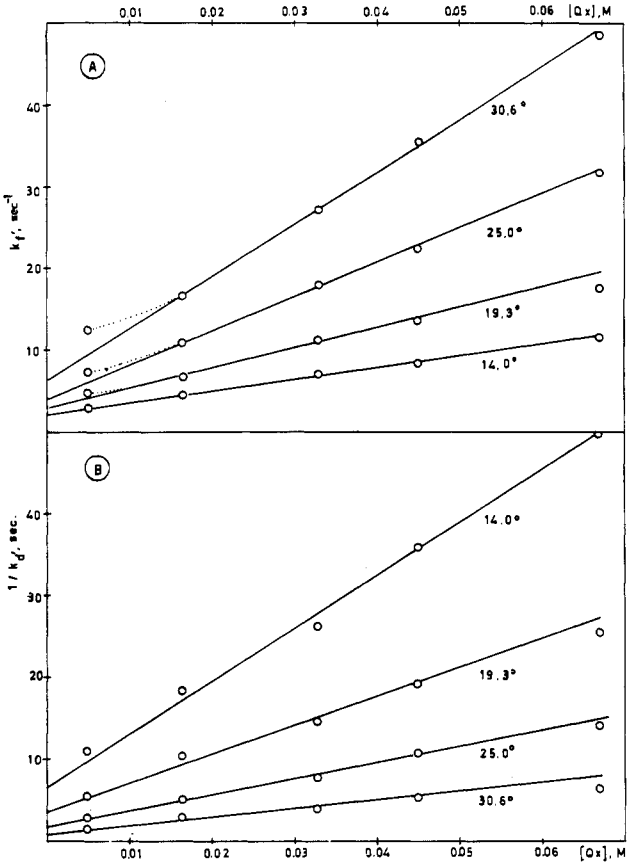

Figure 1. Plots of (A) k_f' vs. [qx] and (B) $1/k_{d'}$ vs. [qx].

$$k_{d'} = \frac{k_6 k_7 [Me_2SO]}{k_{-6}[qx] + k_7[Me_2SO]} \qquad (8)$$

$$\frac{1}{k_{d'}} = \frac{1}{k_6} + \frac{k_{-6}[qx]}{k_6 k_7 [Me_2SO]} \qquad (9)$$

the slopes of these plots and the measured values of k_{-6} and k_{-7}, values of k_6 have been determined as a function of temperature. At 25 °C and μ = 0.10 M, k_6 is 0.62 ± 0.1 s^{-1}. $\Delta H^{\ddagger}$ and $\Delta S^{\ddagger}$ are respectively 19.6 ± 2 kcal mol^{-1} and 4 ± 6 cal mol^{-1} deg^{-1}. Runs 2, 9, 16, and 23 in Table I correspond to independent evaluations of k_6 made by employing a large excess of [Me_2SO] over [qx]. Good agreement was found between values of k_6 so obtained and those found by using eq 9.

Formation Kinetics of the Pyrimidine Complex. Specific rates of formation of the pyrimidine complex from pentacyanoaquaferrate(II), in the presence of excess ligand, were determined at temperatures between 10 and 30 °C at pH 7, in 0.10 M $LiClO_4$ solution. The rate law is rate = k_f[$Fe(CN)_5OH_2^{3-}$][pyr], while k_f is 340 ± 25 M^{-1} s^{-1}, $\Delta H^{\ddagger}$ = 15.5 ± 1 kcal mol^{-1}, and $\Delta S^{\ddagger}$ = 6 ± 3 cal mol^{-1} deg^{-1}.

Dissociation Kinetics of the Pyrimidine Complex. The kinetics of ligand exchange, starting with the pyrimidine complex, were studied by employing Me_2SO as the replacement ligand. The reaction was monitored at 410 nm, following the disappearance of the pyrimidine complex. As shown in Figure 2, the dependence of the pseudo-first-order specific rate of ligand exchange on [Me_2SO] showed rate saturation behavior. Individual points shown in Figure 2 were determined by experiments, while the curve was calculated by substituting appropriate values of the rate constants into eq 13. The form of the curve indicates that the rate-determining step involves

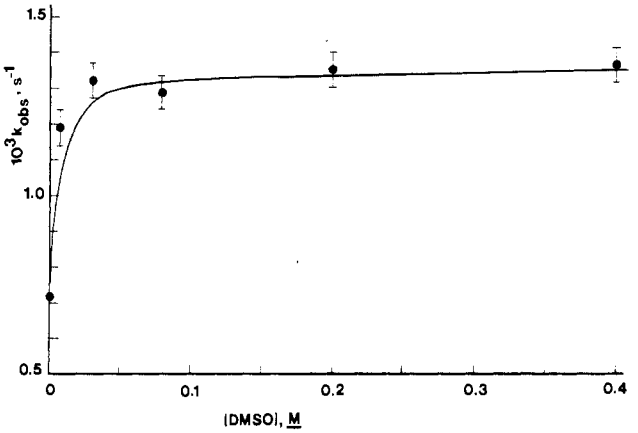

Figure 2. Plot of observed specific rate of substitution, k_{obsd}, for the pyrimidine complex vs. the concentration of Me_2SO, the attacking ligand.

rupture of the iron–heterocycle bond.[3,4]

By use of the mechanism represented in eq 10 and 11 and the steady-state approximation for $[Fe(CN)_5OH_2^{3-}]$, k_{obsd} for the exchange process is related to the rate by eq 12. The quantity $([Fe(CN)_5pyr^{3-}] - [Fe(CN)_5pyr^{3-}]_\infty)$ is the concentration of the pyrimidine complex at time = t minus the concentration at equilibrium.

$$Fe(CN)_5pyr^{3-}(aq) + H_2O \underset{k_{-10}}{\overset{k_{10}}{\rightleftharpoons}} Fe(CN)_5OH_2^{3-}(aq) + pyr \quad (10)$$

$$Fe(CN)_5OH_2^{3-}(aq) + Me_2SO \underset{k_{-11}}{\overset{k_{11}}{\rightleftharpoons}} Fe(CN)_5Me_2SO^{3-}(aq) + H_2O \quad (11)$$

$$\text{rate} = k_{obsd}([Fe(CN)_5pyr^{3-}] - [Fe(CN)_5pyr^{3-}]_\infty) \quad (12)$$

$$k_{obsd} = \frac{k_{10}k_{11}[Me_2SO] + k_{-10}k_{-11}[pyr]}{k_{11}[Me_2SO] + k_{-10}[pyr]} \quad (13)$$

At high $[Me_2SO]$, $k_{obsd} = k_{10}$ and the specific rate of the bond-breaking step can be determined from the limiting rate in Figure 2. At 25 °C, pH 7, and μ = 0.10 M, this value is $(1.3 \pm 0.1) \times 10^{-3}$ s^{-1}. From a temperature dependence study of the limiting rate, $\Delta H^\ddagger = 21.8 \pm 2$ kcal mol^{-1} and $\Delta S^\ddagger = 2 \pm 6$ cal mol^{-1} deg^{-1}.

Redox Properties. A cyclic voltammogram of the quinoxaline complex is given in Figure 3. At moderate scan rates (100–200 mV/s), the one-electron redox couple was found to be reversible, showing a peak-to-peak separation of 60–70 mV. However, the cathodic wave collapsed at the lowest scan rate employed (50 mV/s), suggesting that dissociation of the pentacyanoferrate(III) quinoxaline complex occurs on the time scale of a single, slow scan. E_f for the pentacyano(quinoxaline)ferrate (II/III) couple is measured to be −0.55 V vs. NHE. The pyrimidine complex was studied under similar conditions (22 °C, 0.10 M ($LiClO_4$)), and a value of E_f = −0.52 V was obtained.

Discussion

Values of λ_{max} for several substituted pentacyanoferrate(II) species are compared with the pyrimidine and quinoxaline complexes in Table II. The spectra of these species feature strong ($\epsilon_{max} \sim 5 \times 10^3$ M^{-1} cm^{-1}), low-lying metal-to-ligand charge-transfer bands. One can characterize the primary MLCT* excited states as reduced ligand/oxidized metal species with the energy of the MLCT absorption band governed in each case by the difference between the oxidation potential of the Fe(II) center and the electron affinity of the ligand.

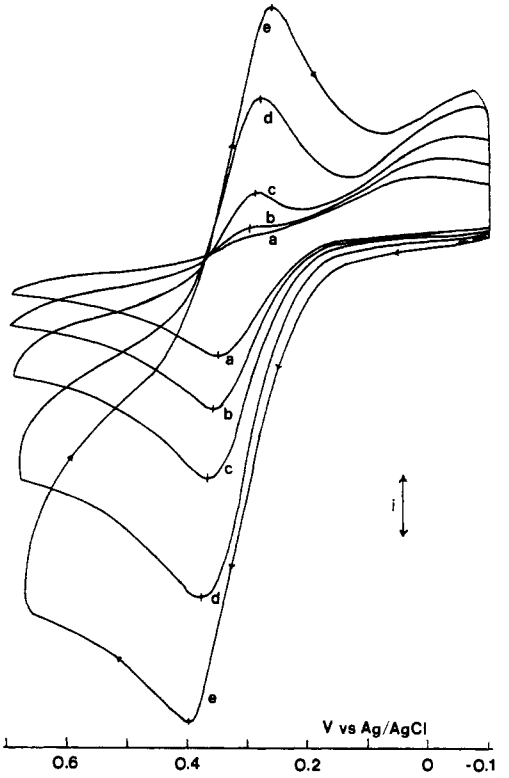

Figure 3. Cyclic voltammograms of the pentacyano(quinoxaline)ferrate(II) complex (4.1×10^{-3} M, 22 °C, 0.1 M $LiClO_4$). Scan rates (mV/s): (a) 50; (b) 100; (c) 200; (d) 500; (e) 1000.

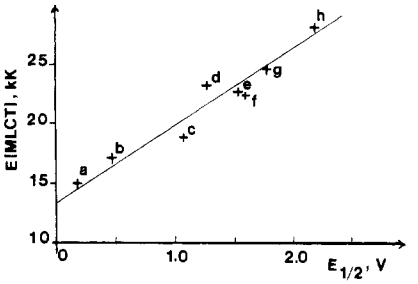

Figure 4. Plot of E(MLCT) for several pentacyano(ligand)ferrate(II) complexes vs. the half-wave reduction potential of the free ligands. Ligands: (a) *N*-methylpyrazinium; (b) *N*-methylpyrimidinium; (c) quinoxaline; (d) 4,4′-bipyridine; (e) *sym*-triazine; (f) pyrazine; (g) pyrimidine; (h) pyridine.

Table II. Formal Potentials and Association Constants for Pentacyanoferrate(II) and -(III) Complexes at 25 °C[a]

ligand	λ_{max}, nm	E_f, V	K_{II}, M^{-1}	K_{III}, M^{-1}	pK_a
4-aminopyridine	320	0.35	1.7×10^5	6.8×10^5	9.17
pyridine	362	0.48	3.3×10^5	9.4×10^3	5.23
pyrimidine	410	0.52	2.5×10^5	1.6×10^3	1.30
isonicotinamide	435	0.50	4.0×10^5	5.2×10^3	3.61
pyrazine	452	0.55	9.0×10^5	1.7×10^3	0.65
quinoxaline	545	0.55	6.9×10^2	1.3	
N-methylpyrazinium	655	0.79	2.0×10^6	4.7×10^{-1}	−5.8

[a] For complexes other than those of pyrimidine and quinoxaline, see ref 10 and the references cited therein.

In the table, one sees that λ_{max} increases in sequence for the complexes of pyridine, pyrimidine, pyrazine, and quinoxaline. As in the series of analogous Ru(II) complexes, E_{MLCT} increases linearly as the half-wave reduction potentials of the heterocycles increase. A plot of E_{MLCT} vs. $E_{1/2}$(free ligand) is given in Figure 4.

Formation Kinetics. For the quinoxaline complex the specific rate of formation, 425 ± 25 M^{-1} s^{-1}, is similar to that for

Scheme I

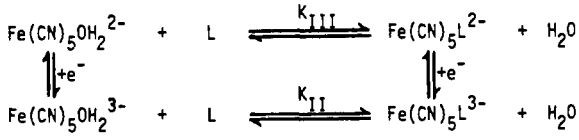

the pyrimidine species, 340 ± 25 M^{-1} s^{-1}. The kinetics of formation agree closely with specific rates of substitution that have been determined for many zero-charge ligands in reaction with $Fe(CN)_5OH_2^{3-}$(aq).[8,10,20] The results are consistent with the view that the substitution process is primarily a dissociative one, in which loss of a coordinated solvent molecule from the inner coordination sphere of iron(II) is rate determining. The steric requirement of the bulky quinoxaline ligand, which manifests itself clearly in the dissociation kinetics, is not observed in the kinetics of formation.

Dissociation Kinetics and Formation Constants. The specific rate of breakage of the iron(II)–pyrimidine bond, (1.3 ± 0.1) × 10^{-3} s^{-1}, is close to that found for the pyridine complex, 1.1 × 10^{-3} s^{-1},[3,10] and 3 times higher than the rate for the pyrazine complex, ca. 4 × 10^{-4} s^{-1}.[3] One can employ the kinetics results to calculate K_{II}, the formation quotient for the pyrimidine complex, eq 14. Here, $K_{II} = k_f/k_d = 2.6 \times 10^5$ M^{-1} when k_{10} is k_d. See the values in Table II.

$$(NC)_5FeOH_2^{3-} + pyr \underset{k_d}{\overset{k_f}{\rightleftharpoons}} (NC)_5Fe(pyr)^{3-}(aq) + H_2O \quad (14)$$

For the quinoxaline complex, $k_d = k_6 = 0.62$ s^{-1}. The complex is considerably more labile than the pyrimidine-substituted species. However, the result is close to the specific rates known for dissociation of several strained complexes of pentacyanoferrate(II). For example, k_d for the 2-cyanopyridine complex is 1.1 s^{-1},[7] the specific rate of dissociation of the N-1 bound isomer of the 2-methylpyrazine complex is estimated as 0.8 s^{-1},[16] and k_d for the hindered N-1 complex of histidine is 0.109 s^{-1}.[8]

From the specific rates of formation and dissociation, one can compute $K_{II} = k_f/k_d = 690$ M^{-1}. K_{II} for quinoxaline is smaller by a factor of 1.3 × 10^3 than that for pyrazine. This factor reflects almost exactly the relationship between the k_d values for the two complexes. From it, one can calculate a "strain" energy of approximately 4.2 kcal mol^{-1} in the iron(II)–quinoxaline interaction.

Stabilities of Pentacyanoferrate(III) Complexes. Like most substituted pentacyanoferrate(II) species, the quinoxaline and pyrimidine complexes are oxidized reversibly at a platinum electrode to produce the corresponding iron(III) species.[14] In Table II, we observe that the values of E_f found for the two complexes in this investigation lie close to those for pyridine and pyrazine.

Utilizing the cycle shown in Scheme I, it is possible to compute K_{III}, the formation quotient for a pentacyanoferrate(III) complex. This is done by employing K_{II} along with the E_f value of the substituted pentacyanoferrate(III/II) couple and $E_f = 0.39$ V for the pentacyanoaquaferrate(III/II) couple. These values are related by eq 15. Substitution of the appropriate quantities yields $K_{III} = 1.6 \times 10^3$ M^{-1} for the pyrimidine complex. In Table III, one notes that this value is somewhat lower than those for pyridine or isonicotinamide but is very close to the value for pyrazine. Toma and Creutz[14] have pointed out that there is a correspondence between ligand pK_a and K_{III}, indicating that the σ-donor capability of the ligand L dominates in determining K_{III}. In contrast, the retrograde dependence of K_{II} on ligand pK_a, also notable in Table II, suggests that other factors govern K_{II}. We have proposed that metal-to-ligand back-bonding is important among these factors.[10]

$$E_f(Fe(CN)_5L^{2-/3-}) = E_f(Fe(CN)_5OH_2^{2-/3-}) + \frac{RT}{F} \ln \frac{K_{II}}{K_{III}} \quad (15)$$

For the quinoxaline complex, K_{III} is only 1.3 M^{-1}. The value is especially low, comparable to $K_{III} = 0.47$ M^{-1} for the *N*-methylpyrazinium ligand, which is positively charged and a very poor Brønsted base. In comparison with the value of K_{III} for pyrazine, Table II shows the sterically strained pentacyano(quinoxaline)ferrate(III) complex to be less stable, by a factor of ca. 1300, with respect to aquation.

Our cyclic voltammetry experiments showed a loss of reversibility at slow scan rate that probably was caused by loss of the heterocycle from pentacyano(quinoxaline)iron(III). We estimate that the rate of ligand loss was ca. 0.1 s^{-1} under the experimental conditions. If, as we have found, K_{III} is close to unity and k_d is ca. 0.1 s^{-1}, the microscopic reversibility relationship $k_f = K_{III}k_d$ requires a value of $k_f \approx 0.1$ s^{-1}. To our knowledge, accurate studies of the rate of substitution for H_2O in $Fe(CN)_5OH_2^{2-}$ have not yet been performed. Thus, this estimate is subject to direct verification.

Acknowledgment. A.L.C. gratefully acknowledges fellowship support from the Universidade Federal do Ceará and from CAPES/PICD.

Registry No. I, 289-95-2; II, 91-19-0; $Fe(CN)_5OH_2^{3-}$, 18497-51-3; $Fe(CN)_5pyr^{3-}$, 86260-12-0; $Fe(CN)_5qx^{3-}$, 86632-36-2; Me_2SO, 67-68-5.